Journal of Applied Pharmaceutical Science Vol. 13(03), pp 023-035, March, 2023
Available online at http://www.japsonline.com
DOI: 10.7324/JAPS.2023.62346
ISSN 2231-3354

# Physically cross-linked PVA-quaternized chitosan-Ag NPs composite hydrogel membranes for potential topical wound healing applications: Synthesis, physicochemical properties, and *in vitro* bioevaluation

El-Refaie S. Kenawy[1], Elbadawy A. Kamoun[2,3*], Samia M. Elsigeny[4], Samira Haikal[1], Ashraf A. El-Shehawy[4], Yehia A. G. Mahmoud[1]

[1]Chemistry Department, Faculty of Science, Tanta University, Tanta, Egypt.
[2]Polymeric Materials Research Dep., Advanced Technology and New Materials Research Institute, City of Scientific Research and Technological Applications (SRTA-City), Alexandria 21934, Egypt.
[3]Nanotechnology Research Center (NTRC), The British University in Egypt (BUE), Cairo, Egypt.
[4]Chemistry Department,Faculty of Science, Kafr Elsheikh University, Kafr El-Sheikh, Egypt.

**ARTICLE INFO**

Received on: 18/06/2022
Accepted on: 06/11/2022
Available Online: 04/03/2023

***Key words:***
PVA-quaternized chitosan, Ag NPs, freezing–thawing cycle, hydrogel membranes.

**ABSTRACT**

Physically cross-linked composite hydrogel membranes composed of different ratios of polyvinyl alcohol- (PVA-) grafted modified chitosan (Cs) with glycidyltrimethylammonium chloride (GTMAC) loaded with Ag nanoparticles as an active ingredient were synthesized by the freezing-thawing (F-T) cycle technique. F-T cycles were conducted repetitively three times to guarantee PVA-Cs chains entanglement occurring. The reactants, membrane composition, and cross-linking process were verified and characterized by several instrumental analyses. The physicochemical properties of the PVA-Cs-g-GTMAC hydrogel membrane, such as swelling ratio, mechanical properties, gel fraction % (GF %), hydrolytic degradation, and thermal stability, were discussed in detail. The results revealed that, with increasing of the Cs-g-GTMAC content in the hydrogel membranes, the swelling ratio, mechanical properties, and hydrolytic degradation of the cross-linked membranes increased clearly; however, GF % decreased progressively. Furthermore, in order to assess *in vitro* bioevaluation of the tested composite membranes, e.g., cytotoxicity and antimicrobial studies against the HFB-4 cell line and both *Staphylococcus aureus* and *Escherichia coli*, respectively, were assessed using the MTT assay and disc diffusion method, respectively. Notably, all tested composed hydrogels exhibited high cell viability % after different incubation times and varied hydrogel concentrations. The findings referred to the idea that prepared hydrogel membranes could be professionally employed as antibacterial biomaterials/dressings for wound healing purposes.

## INTRODUCTION

One of the preferable conditions for faster and better healing is to keep the wound bed area moist (Caló *et al*., 2015). Therefore, wound dressings must offer maintaining of a wet environment through absorbing the excess exudates and fluids from the wound surface in addition to avoiding microbial growth. However, traditional wound dressing, e.g., cotton and gauze, cannot provide this condition because the cotton absorbs all wound's exudates, causing a very dried wound surface, besides adhering to the new formed epithelial cells on the cotton, causing removal of strong pains and a slow healing process in the patient (Kamoun *et al*., 2015a). Accordingly, using hydrogel membranes shall provide a more convenient route for wound dressing. In this

*Corresponding Author
*Elbadawy A. Kamoun, City of Scientific Research and Technological Applications, Alexandria, Egypt.*
*E-mail: badawykamoun @ yahoo.com*

light, a hydrogel is a promising biomaterial for wound dressing materials (Kamoun *et al*., 2017). A physical route of cross-linking such as repetitive freezing–thawing (F-T) cycles is more suitable for medical needs, owing to its solvent-free composition, biocompatibility, and nontoxicity, than the traditional chemical cross-linking methods. In addition, the physically prepared gel has high water uptake and achievable physical characteristics, e.g., elastic nature, compared to chemically cross-linked hydrogels (Kamoun *et al*., 2015b).

Polyvinyl alcohol (PVA) is a water-soluble polymer popularly utilized in biomedical applications. Also, it is used for several pharmaceutical purposes, owing to its benefits such as being noncarcinogenic, nontoxic, bioadhesive, and biodegradable with the simplicity of film-forming ability (Hassan *et al*., 2018a; Tang *et al*., 2019). However, the utilization of PVA alone forms a stiff membrane with inadequate elasticity, which restricts its use as a wound dressing polymeric membrane (Simões *et al*., 2018). Therefore, PVA is used preferably with blending with other natural polymers for improving the overall biological properties of the resultant cross-linked blend membranes.

Chitosan (Cs), poly-*β*-(1-4)-*D*-glucosamine, is a cationic marine polysaccharide prepared from a deacetylated derivative of chitin (Martins *et al*., 2014). Recently, Cs has been regularly utilized as an anticancer agent, plant disease resistance promoter, wound healing agent, and antimicrobial agent as it possesses exclusive properties, e.g., nontoxicity, high antimicrobial activity, and good biodegradability (Al Ghamdi *et al*., 2017). However, Cs has poor water solubility at pH ~6.5; consequently, its activities are very limited in acidic conditions (Liu, 2015). Hence, Cs solubility could be enhanced by its chemical modification (Cheah *et al*., 2019). The derivatization of Cs throughout quaternary ammonium compounds could extend a better antibacterial efficacy than pure Cs (Cai *et al*., 2015). Hence, Cs could be derivatized with quaternary ammonium salt [i.e., glycidyltrimethylammonium chloride (GTMAC)] to procedure quaternized Cs films for solving the solubility problem of pure Cs at medium values of pH.

Many active ingredients, e.g., metal oxides, carbon-based materials, vitamins, drugs, and silver or gold nanoparticles, were incorporated into hydrogel membranes for enhancing their bioevaluation. Silver is a good antimicrobial agent with a reported high efficiency besides its wide-spectrum resistance to bacterial, viral, and fungal infections (Paladini and Pollini, 2019), where silver nanoparticles have significant novel promising properties (Wilkinson *et al*., 2011), such as their nanoscale size; Ag nanoparticles (Ag NPs) offered new horizons toward novel approaches in controlling infections of chronic ulcers, diabetic populations and chronic wounds causing faster healing process for its unique properties as moisturizing agent for wound bed, damages formed thin biofilm by bacteria, acts to improve oxygenation, angiogenesis and granulation on wounds, aid for removing of debris and dirt, does not affect normal flora, reduce odors and has bactericidal effects on common pathogens like *Escherichia coli*, *Pseudomonas*, *Staphylococcus* (Suhas and Manvi, 2018).

It has been reported that Cs-g-GTMAC has stronger antibacterial properties than Cs itself and a generally positive charged conjugate showed improved properties paralleled to unmodified Cs (Chi *et al*., 2007; Shariatinia and Jalali, 2018; Vinsova and Vavrikova, 2011). Therefore, as shown, there have been separate studies on both Cs-g-GTMAC and nanosilver while in our study we are combining both of them aiming to have the benefits of them together and furthermore them enhancing each other.

This work aims to prepare and characterize potential topical wound dressings as self- sterilized biomaterials based on physically cross-linked PVA-Cs-g-GTMAC hydrogel membranes. The physicochemical properties of PVA were improved by blending with Cs-g-GTMAC, while the solubility and antimicrobial activities of pure Cs were enhanced by modification with GTMAC. Meanwhile, Ag NPs were loaded into PVA-Cs-g-GTMAC hydrogel membranes for improving the antimicrobial spectrum and biocompatibility properties of the composite membrane. In addition, the physical cross-linking (F-T) method was utilized for avoiding the risk of using traditional chemical cross-linkers due to their common toxic effects.

## MATERIALS AND METHODS

### Materials

PVA (MW ~72,000 g/mol; 95% hydrolyzed) was attained via ADVENT CHEMBIO PVT LTD (Mumbai, India). Cs was purchased from Carl Roth (Germany). GTMAC, silver nitrate, trisodium citrate, and ascorbic acid were acquired from Sigma-Aldrich (Germany). Distilled water was utilized in this work for membrane fabrication and further experiments.

### Experimental part

#### *Modification of Cs with GTMAC*

Cs was chemically modified to quaternized Cs agreeing to the route of Abdelaal et al. (2013). In brief, 0.4 ml of GTMAC was mixed with a suspension solution composed of 0.5 g of Cs in 50 ml of distilled water with constant stirring for 24 hours at 80°C. Acetone was added wisely to the Cs solution mixture to stop the reaction and to precipitate the modified Cs, as shown in Scheme 1. The suspended beads were converted from translucent into small yellowish-white beads after the reaction ended. The produced Cs-g-GTMAC was detached by filtration and dried at 60°C under vacuum for 24 hours. The resultant Cs-g-GTMAC was washed three times with acetone to remove the excess of the unreacted GTMAC. The obtained Cs-g-GTMAC copolymer was extra-dried in a vacuum oven at 50°C for 6 hours and stored at 4°C for further experiments.

#### *Preparation of Ag NPs in situ*

Ag NPs were synthesized by a sodium citrate reduction reaction of $AgNO_3$, as published elsewhere (Jin *et al*., 2003). In brief, 18 mg of $AgNO_3$ was dissolved in 100 ml of distilled water, and the solution was kept for boiling for a half hour in a closed system. A solution of 1% trisodium citrate (2 ml) was added, and the latter mixture was kept under boiling for a further *ca*. 1 hour. The total mixture was attuned to 500 ml, while the obtained Ag sols became a greenish-yellow product.

#### *Preparation of PVA-Cs-g-GTMAC loaded-Ag composite hydrogel membranes*

PVA-Cs-g-GTMAC cross-linked hydrogel membranes were attained by an F-T cycle. A mixture composed of 10% (w/v) of PVA and Cs-g-GTMAC (0%, 10%, 20%, and 30%, w/v) were

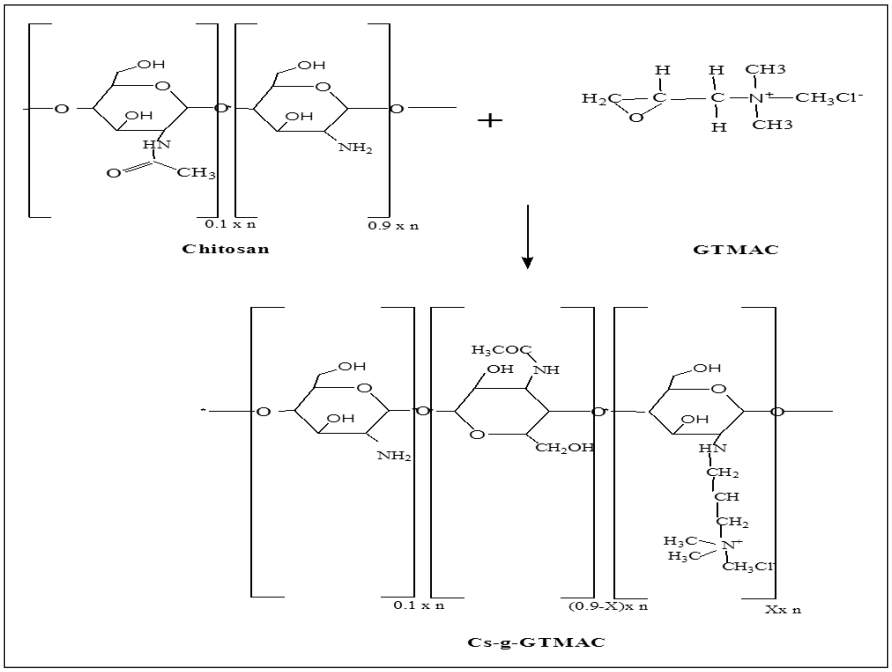


**Scheme 1.** Reaction mechanism of modification of Cs with GTMAC.

dissolved in distilled water, and then 1% (v/v) of acetic acid and 0% or 5% (w/v) of the Ag NPs solution were well mixed with the polymer solution. The polymer-Ag solution was mixed carefully in water bath sonication for a further 1 hour and poured into a plastic Petri dish through the solution-casting method. The mixture solution was then frozen at −20°C for 12 hours and afterward was thawed at RT for 2 hours; the F-T cycle was carried out three times. Afterward, the formed membranes were thermally treated at 60°C for 12 hours for obtaining dried cross-linked membranes.

## Methods

### *Water uptake (%)*

The swelling ration (%) or water uptake (%) of the PVA-Cs-g-GTMAC membranes was first cut into (2 × 2 cm) pieces and dried at 60°C in an oven for 6 hours; the weight of the dried sample was then determined ($W_e$). The dried membranes were immersed in distilled water and kept at 37°C and then weighed ($W_s$) again at precise interval times. The swelling ratio of the PVA-Cs-g-GTMAC membranes was calculated *via* the following equation (Yang *et al*., 2008a):

$$\text{water uptake (\%)} = (W_s - W_e / W_e) \times 100, \quad (1)$$

where $W_s$ is the mass of the swelled membrane and $W_e$ is the weight of the dried membrane.

### *Gel fraction (%) (GF %)*

The prepared PVA-Cs-g-GTMAC membranes were first dried under room conditions for 24 hours before being dried again at 60°C in an oven for 24 hours and weighed ($W_0$). The dried membranes were kept in distilled water for 24 hours up to reaching the equilibrium swelling weight ($W_s$). The hydrogel membranes were then dried at 60°C in an oven and weighed again ($W_e$). The GF % was determined by the given formula of Yang *et al*. (2008b):

$$\text{GF (\%)} = (W_e / W_0) \times 100, \quad (2)$$

where $W_e$ is the mass of the swelled sample after drying and $W_0$ is the dried mass of the membrane.

### *Hydrolytic degradation*

The degradation rates or weight loss (%) was measured using a method reported elsewhere (Xiao and Zhou, 2003). Briefly, 2 × 2 (cm) dried membranes were weighed and soaked in 10 ml phosphate-buffered saline (PBS) (0.1 M, pH 7.4) at 37°C. The membranes were eliminated at interval times, then blotted with soft papers for removing excess water, and dried under room conditions, and the mass was weighed at precise time intervals, as well. The weight loss (%) was calculated using the following equation, where $W_i$ is the original mass of the membrane and $W_f$ is each piece eliminated from the medium, dried in a vacuum oven, and then weighed:

$$\text{weight loss (\%)} = (W_i - W_f)/W_i \times 100. \quad (3)$$

## Bioevaluation tests

### *Antimicrobial activity test*

The antibacterial activities of the tested samples at different cinnamaldehyde concentrations were assessed by following the lately reported procedures of Valgas *et al*. (2007), Kenawy *et al*. (2019), and Hassan *et al*. (2018a), where the *E. coli*. (NCTC10418) and *Staphylococcus aureus* [American Type Culture Collection (ATCC) 25923] isolates used in the *in vitro* test of antibacterial activity were standardized by the ATCC. Typically, the refreshed bacteria suspensions were diluted up to 100 times with a 1% LB broth medium. A 100 µl diluted suspension was cultivated in 10 ml of a tryptone medium containing 0.1 g of the tested membranes, followed by sterilization at 120°C for 10 minutes. Thus, the mixture was kept with shaking for 18 hours at

37°C, and the growth inhibition % of bacteria was identified by assessment of the absorbance of the culture medium at 600 nm by a spectrophotometer. The inhibition (%) was considered using the equation

$$\text{inhibition (\%)} = (A_a\text{-}A_b) / A_a \times 100, \quad (4)$$

where $A_b$ and $A_a$ are the absorbances of the bacterial culture without/with the tested samples, respectively.

### *In vitro cytotoxicity test*

The effect of the prepared compounds [PVA, PVA+Ag, PVA+Cs, PVA+Cs-g-GTMAC+Ag (90: 10), PVA+Cs-g-GTMAC+Ag (80: 20), and PVA+Cs-g-GTMAC+Ag (70: 30)] on cell viability of the HFB-4 (normal human skin melanocyte) cells was assayed using the colorimetric MTT cell viability method (El-Fakharany *et al*., 2020; Mosmann, 1983). All tested compounds at discs' weights of 1.0, 2.0, 3.0, 4.0, and 5.0 mg/ml in triplicate were added to the attached cells in sterile 24-well flat-bottom plates at a density of $1.0 \times 10^5$ cells/well and incubated for 2, 4, and 6 days at 37°C in a 5% $CO_2$ incubator. The cell viability % was accounted for by the following formula:

$$\text{relative cell viability (\%)} = (X)_{test} / (Y)_{control} \times 100\ (\%). \quad (5)$$

### Characterization

The preparation of the samples for each instrumental characterization was discussed in detail in the Supplementary Materials, where the tested samples were analyzed by FT-IR, SEM, TEM, mechanical properties, and thermal stability (Kamoun and Menzel 2012).

## RESULTS AND DISCUSSION

### Preparation and morphology of Ag NPs

Ag colloids were utilized as templates which were synthesized using a sodium citrate reduction reaction of an $AgNO_3$ solution to create faceted particles, showing a range of altered morphologies, with a ranged size scale of ~30–60 nm, as shown by TEM images (Fig. 1). The TEM images display the spherical shape of the obtained Ag NPs with an average size of ~50 nm in diameter.

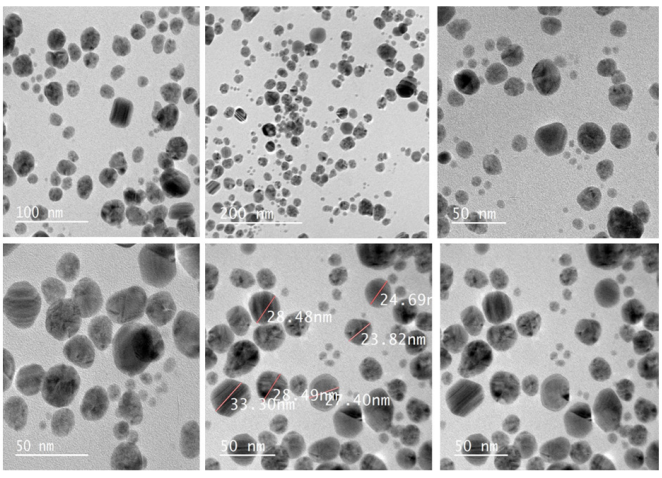


**Figure 1.** TEM images of Ag NPs with different magnification scale (50, 100, and 200 nm) (up) and average diameter size of Ag NPs was determined with magnification scale 50 nm (down).

It was detected that the core portions of Ag NPs were observed to be darker than their edges, owing to a changed thickness of silver along the path of the electron beam. The as-synthesized Ag colloids showed a greenish-yellow tint, and its destruction spectrum chart displays a sharp peak centered at 426 nm (Fig. S1, Supplementary Material). These findings are consistent with the obtained results of Kamel *et al*. (2019), who discussed a selective detection of metal ions as silver.

### *FT-IR of Cs-g-GTMAC composite hydrogel membranes*

Figure 2 shows the FT-IR spectra of PVA, Cs, GTMAC, and Cs-g-GTMAC. The supreme striking alteration between two spectra is the characteristic peak located at $\nu$ 1,488 $cm^{-1}$ in GTMAC and Cs-g-GTMAC, which matches an asymmetric angular bending of -$CH_3$ groups of quaternary hydrogen (Liu, 2015). Thus, this peak was not identified in the IR spectrum corresponding to the original Cs or PVA. Meanwhile, N–H bending at $\nu$ 1,600 $cm^{-1}$ of the primary amine was observed to be weak in GTMAC or Cs-g-GTMAC, owing to the change of the primary amine to the secondary aliphatic amine, compared to its presence in Cs (Chi *et al*., 2007) (Fig. 2).

For evidencing the quaternization reaction of Cs into Cs-g-GTMAC, the infrared spectrum of Cs-g-GTMAC is presented in Figure 2. The spectrum displayed a clear absorption peak at $\nu$ 1,607 $cm^{-1}$, equivalent to the C-N-C bending vibration of Cs-g-GTMAC branches. Also, the C=O stretching vibration of the amide group of chitin segments (i.e., traces of the original source of Cs), occurring at $\nu$ 1,731 $cm^{-1}$, can be regarded as an invariant peak, which can be found in both Cs and GTMAC-Cs copolymers. The absorption peak at $\nu$ 2,938 $cm^{-1}$ was attributed to the -C-H stretching vibration of the -$CH_2$ or -$CH_3$ groups, while a broad peak centered at $\nu$ 3,317 $cm^{-1}$ represented the combined O-H stretching vibration and N-H stretching vibration. For further evidence, the entanglement via freeze-thawed PVA is described as C-H broad alkyl stretching at $\nu$ 2,850 $cm^{-1}$ and the –OH group of free unreacted alcohol (nonbonded –OH) strong stretching at $\nu$ 3,650–3,590 $cm^{-1}$, hydrogen bond bands (bonded OH) at $\nu$ 3,600–3,200 $cm^{-1}$, and the sharp absorption peak at $\nu$ 1,150 $cm^{-1}$ as a sign of the IR spectrum of PVA (Kenawy *et al*., 2014).

### Physicochemical properties

#### *Swelling study (%)*

Figure 3 represents the swelling ratio (%) of the PVA-Cs-g-GTMAC hydrogel membranes at different ratios of membrane compositions. As noticed, the swelling ratio (%) increased closely with increasing the content of Cs-g-GTMAC against the PVA content in the hydrogel membranes. This is because the Cs derivative possesses a strong ability to form hydrogen bonding in water as a swelling surrounding, whereas, in the absence of Cs-g-GTMAC (i.e., 100% of PVA), a highly cross-linked and compressed structure of PVA hydrogel membranes was obtained, which might not keep water in the membranes, resulting in a low swelling ability with water uptake (%) of about 280%. Once the Cs-

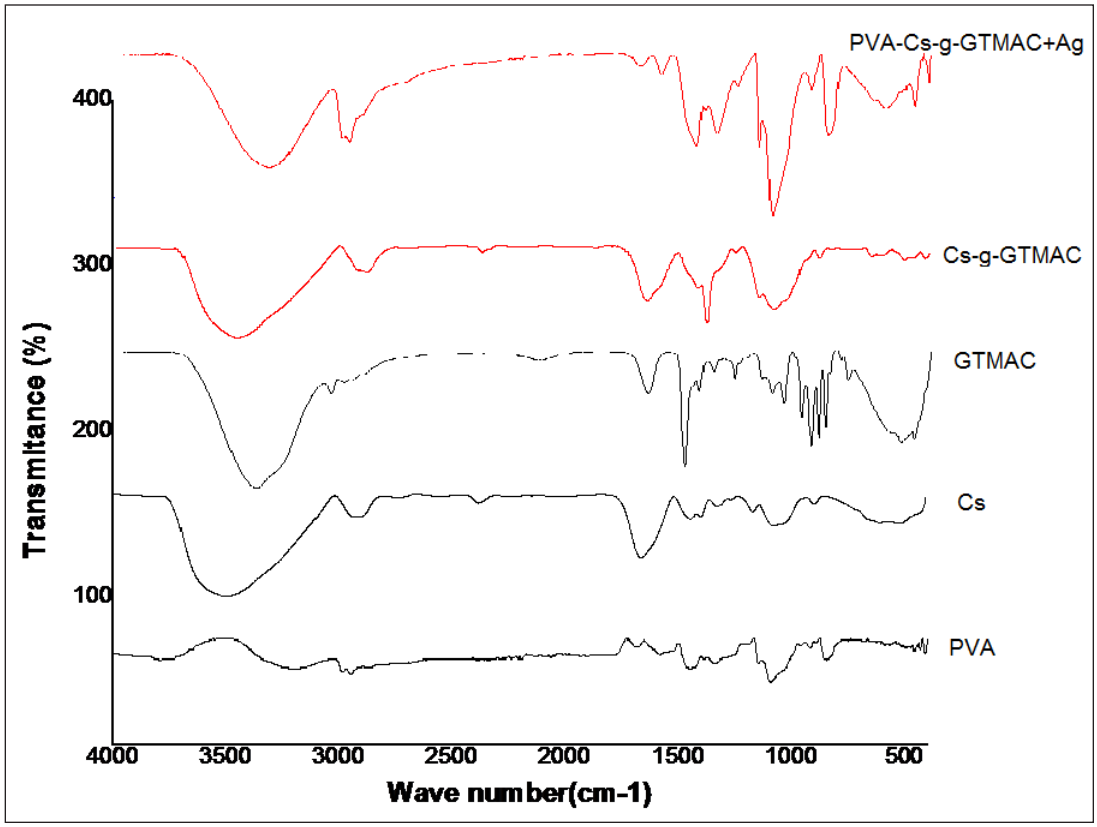


**Figure 2.** FTIR spectra of PVA, Cs, GTMAC, Cs-g-GTMAC, and PVA-Cs-g-GTMAC (80:20) +Ag NPs.

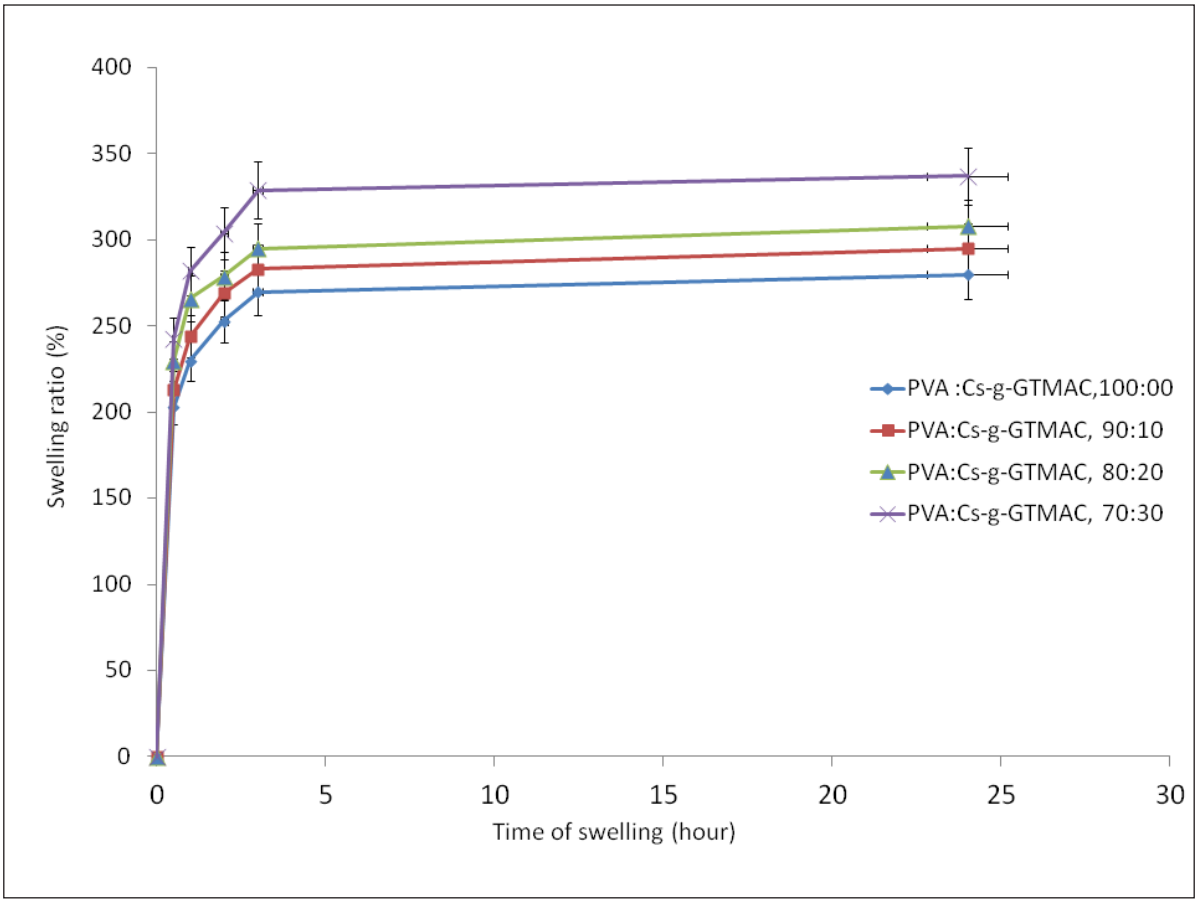


**Figure 3.** Effect of different composition of membranes (PVA-Cs-g-GTMAC-Ag) on swelling ratio of physically crosslinked membranes.

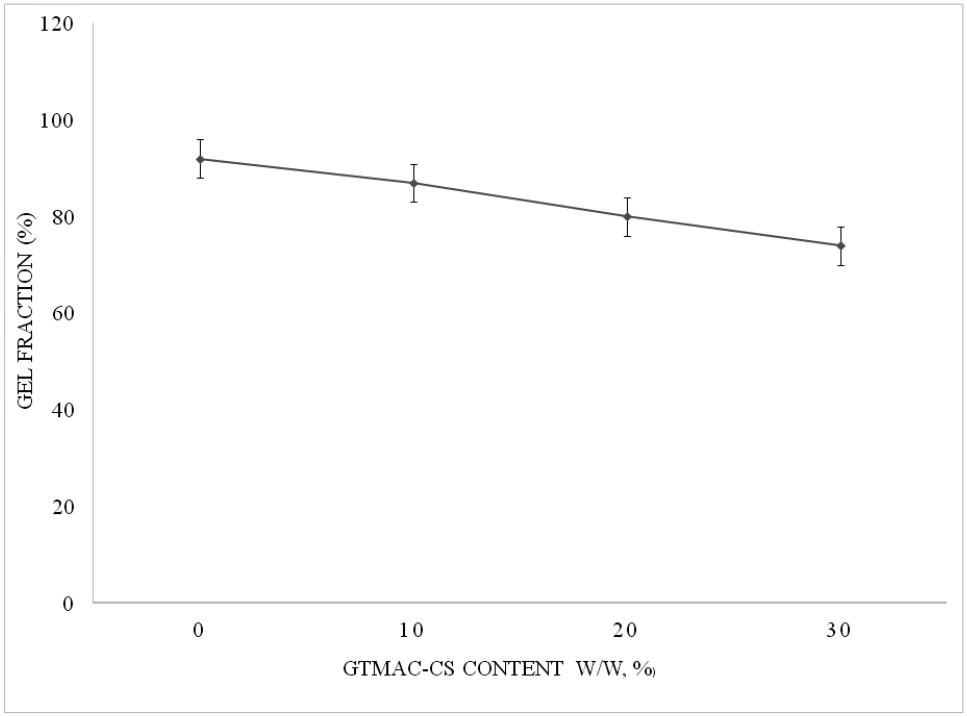


**Figure 4.** Effect of Cs-g-GTMAC content in PVA hydrogel membranes on GF.

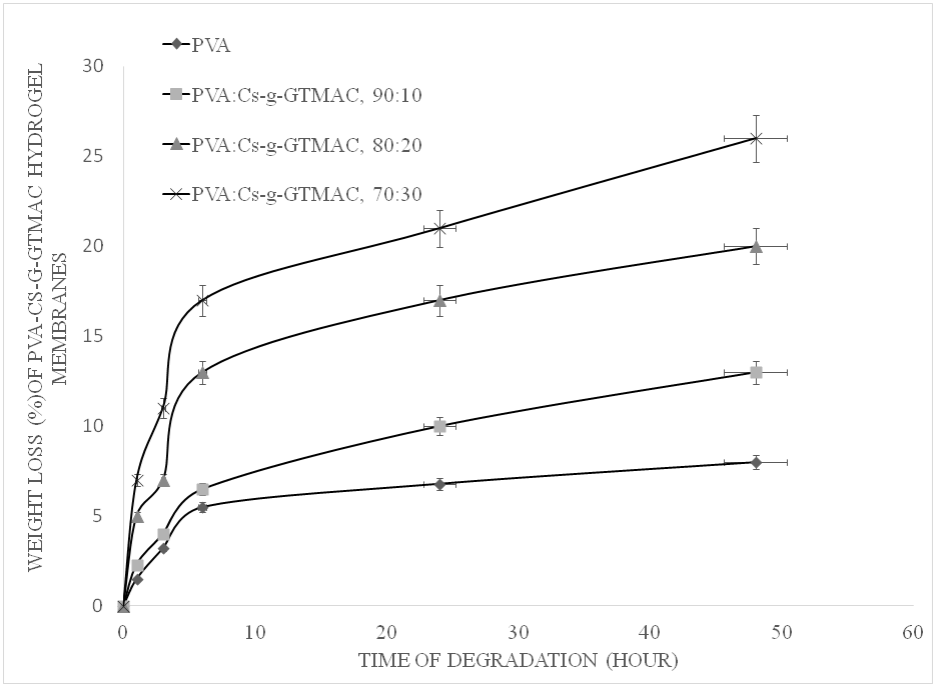


**Figure 5.** Effect of Cs-g-GTMAC contents on weight loss (%) of PVA-Cs-g-GTMAC hydrogel membranes after different degrading times in PBS (0.1 M, pH 7.4, at 37oC).

g-GTMAC content in the hydrogel membrane increased to 30%, the water uptake % increased sharply to 340%. Thus, increasing the content of Cs-g-GTMAC in the PVA membranes notably increased the wettability of the membranes. These observations depended on the previous results of Afshar et al. (2020), where sodium alginate/PVA-loaded Cs NPs membranes were prepared and tested as a drug delivery system.

### *Gel fraction (%)*

Figure 4 illustrates the GF of the PVA hydrogel membranes with different Cs-g-GTMAC content. The results showed that with increasing the Cs-g-GTMAC content the GF of the prepared membranes decreased. The repeated F-T cycles resulted in entangled PVA-Cs-g-GTMAC polymer hydrogel membranes. However, increasing the Cs-g-GTMAC content in the PVA hydrogel might decrease the cross-linking degree, and the gelation process decreases significantly. In the absence of Cs-g-GTMAC, the GF % reached the high value of about 92%. This result agreed with the published findings of Kamoun *et al*. (2014), where GF (%) of PVA-HA blended membranes declined with increasing the HA content in membrane structure.

### *Hydrolytic degradation*

Figure 5 shows the hydrolytic degradation of PVA membranes with different Cs-g-GTMAC content in PBS. The presented data indicates that the hydrolytic degradation of the PVA membrane increases with high Cs-g-GTMAC content in membrane composition. This might be owing to the fact that the degradation of the PVA-Cs-g-GTMAC membranes might result from a cleavage of cross-linking segments of PVA. These results are ascribed to the fact that the degradation of PVA is somewhat low, whereas the degradation of PVA-Cs-g-GTMAC is observed to be somewhat high, as well. Moreover, PVA and Cs-g-GTMAC are nontoxic; the PVA-Cs-g-GTMAC hydrogel and its degradation as byproducts might be proposed as being nontoxic biomaterials, too. The latter findings are consistent with the reported results by Kenawy *et al*. (2014), where the hydrolytic degradation rate of PVA-HES blended membranes increased progressively with increasing of the HES content in the PVA hydrogel membranes.

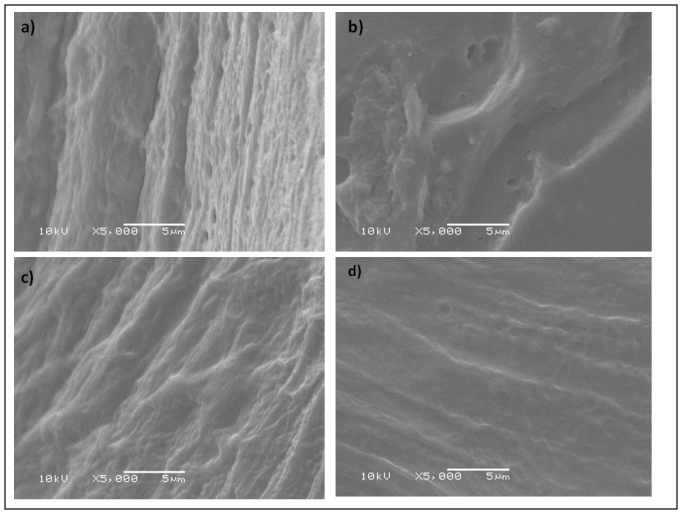


**Figure 6.** SEM images of physically-cross-linked hydrogel membranes composed of (a) PVA (100%) -Ag, (b) PVA-Cs-g-GTMAC-Ag (90:10), (c) PVA-Cs-g-GTMAC-Ag (80:20), and (d) PVA-Cs-g-GTMAC-Ag (70:30), (original magnification of all images ×5,000 at 10 Kv).

## Characterization

### *Surface morphology investigation*

The surface morphology of the PVA membranes against diverse portions of Cs-g-GTMAC is presented in Figure 6. As displayed in SEM images, the absence of Cs-g-GTMAC displays a very uniform, smooth, compacted, compressed, and nonporous shape-surface structure. Nevertheless, the incorporation of Cs-g-GTMAC into the PVA hydrogel in different potions (10, 20, and 30%, w/v) provided very tiny pores at the surface, where these pores notably increase clearly with increasing of the Cs-g-GTMAC contents in the membranes. The morphological changes might be attributed to the existing good homogeneity and hydrophilicity or high miscibility degree between two constituents of the composite membranes (i.e., PVA and Cs-g-GTMAC). The result in the ordered crystalline phase and uniform shape structure in the case of 0% of Cs-g-GTMAC is owing to the highly entangled PVA and the disordered crystalline phase of the PVA membranes blended with different portions of Cs-g-GTMAC. The current SEM investigation agreed with the reported findings of Figueroa-Pizano *et al*. (2018) on PVA-CS hydrogel blend membranes.

### *Mechanical stability*

The mechanical properties of the PVA-Cs-g-GTMAC-Ag composite hydrogels were tested at varied membrane composition ratios between PVA and Cs-g-GTMAC; the data are itemized in Table 1. Elongation to break of the physical hydrogel membranes was enhanced from 60% to 130%, 145%, and 220% due to the incorporation of Cs-g-GTMAC from 0% to 10%, 20%, and 30%, respectively. The elongation % and elasticity improvement of the hydrogel membranes might be ascribed to the increase of the Cs-g-GTMAC portion in the membranes' composition due to its high hydrophilicity and easy homogeneity compared to the PVA membranes. Similarly, both Young's modulus and maximum stress of the hydrogel membranes improved with the gradual incorporation of Cs-g-GTMAC into the hydrogel membranes (Table 1). It was observed that elasticity or elongation to break (%) and flexibility of the PVA-Cs-g-GTMAC composite hydrogels improved significantly by the incorporation of Cs-g-GTMAC; accordingly, the currently prepared membranes are recommended as a dressing biomaterial

**Table 1.** Effect of membrane composition on mechanical properties of physically cross-linked PVA-Cs-GTMAC-Ag hydrogel membranes.

| Membrane composition (PVA: Cs-GTMAC) (%) | Maximum stress ($N/mm^2$) | Elongation-to- break (%) | Young's Modulus (M Pa) |
|---|---|---|---|
| 100:0 | 6 | 60 | 34 |
| 90:10 | 15 | 130 | 40 |
| 80:20 | 22 | 145 | 48 |
| 70:30 | 25 | 220 | 55 |

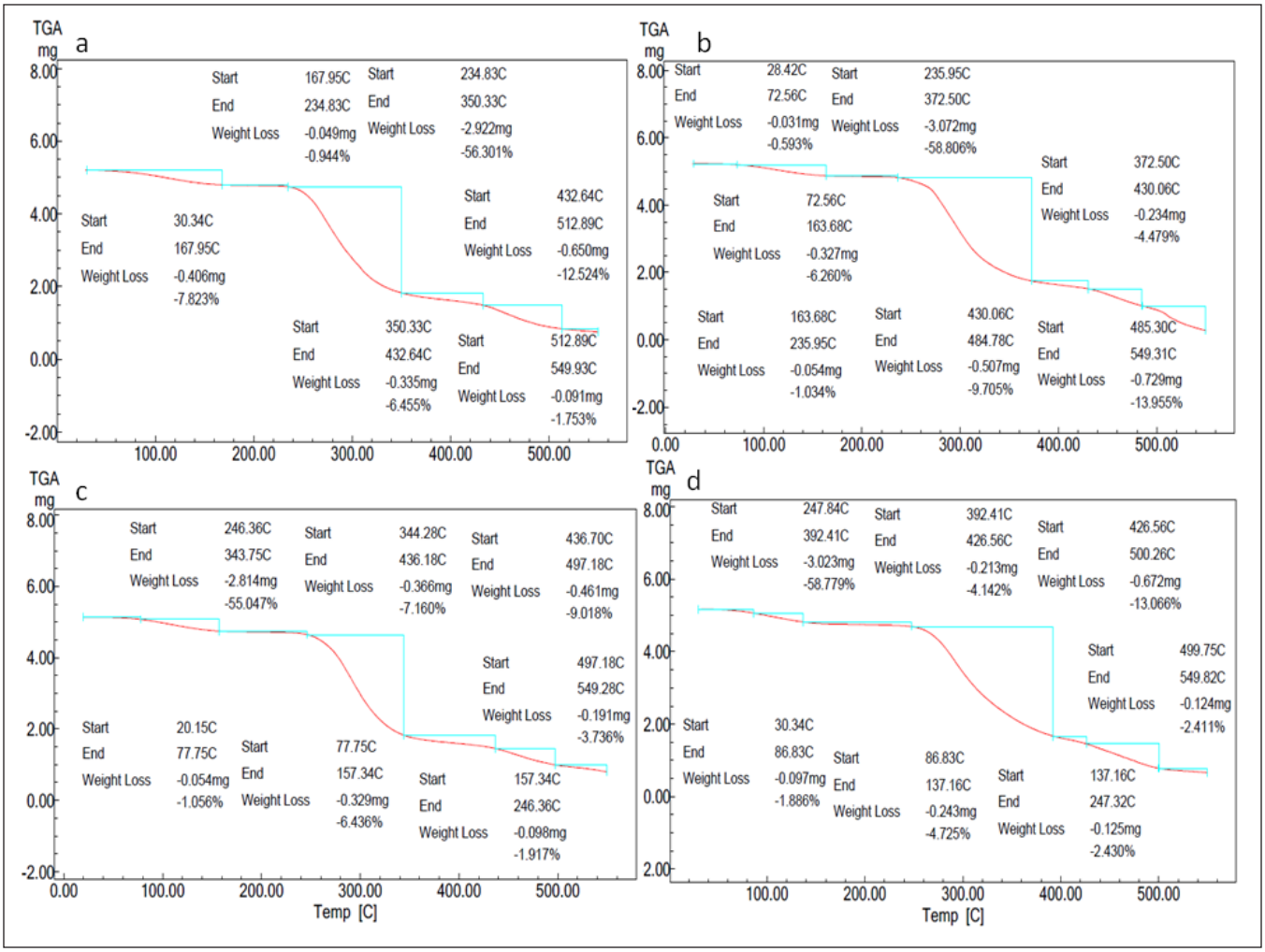


**Figure 7.** TGA thermographs of physically-cross-linked hydrogel membranes composed of (a) PVA (100%)-Ag NPs, (b) PVA-Cs-g-GTMAC-Ag NPs (90:10), (c) PVA-Cs-g-GTMAC-Ag NPs (80:20), and (d) PVA-Cs-g-GTMAC-Ag NPs (70:30).

**Table 2.** TGA results of physically-cross-linked PVA-Cs-GTMAC-Ag hydrogel membranes as function of hydrogel membranes composition ratios between (PVA: Cs-g-GTMAC).

| Membrane composition (PVA: Cs-GTMAC) (%) | $T_{onset}$ (°C) | $T_{50\%}$ (°C) | Second Decomposition stage (°C) | Third Decomposition stage (°C) |
|---|---|---|---|---|
| 100:0 | 234 | 345 | 234–350 | 350–435 |
| 90:10 | 235 | 348 | 235–375 | 375–485 |
| 80:20 | 246 | 350 | 246–344 | 345–549 |
| 70:30 | 247 | 361 | 247–395 | 396–500 |

**Table 3.** Antimicrobial activity test results of composite hydrogel membranes composition.

| Sample | | *Staphylococcus In. %* | *Escherichia coli In %* |
|---|---|---|---|
| PVA | | 3.5 | 2 |
| PVA+ Ag | | 48 | 55 |
| PVA+Cs | (80:20) | 58 | 50 |
| PVA+Cs-g-GTMAC+Ag | ( 90:10) | 61 | 58 |
| PVA+Cs-g-GTMAC+Ag | (80:20) | 65 | 63 |
| PVA+Cs-g-GTMAC+Ag | (70:30) | 80 | 70 |

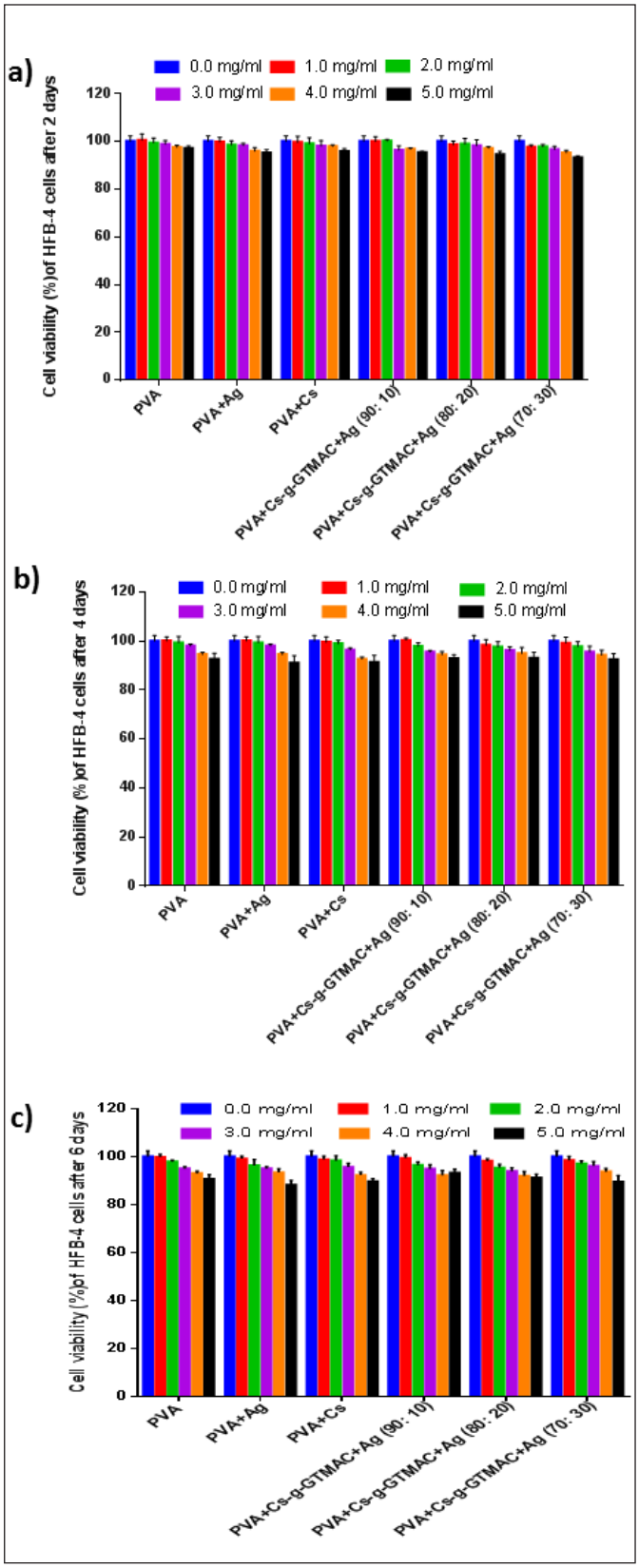


**Figure 8.** HFB-4 cell viability (%) of different hydrogel membranes composed of PVA (100%)-Ag, PVA-Cs-g-GTMAC-Ag (90:10), PVA-Cs-g-GTMAC-Ag (80:20), and PVA-Cs-g-GTMAC-Ag (70:30) after (2, 4, and 6 days) of incubation time.

for wounds and burns. These obtained results are consistent with Zhao *et al*. (2003), where elongation at break and tensile strength of PVA/CM-Cs hydrogel increased with increasing of the CM-Cs content in hybrid membranes.

### *Thermal stability*

The thermal properties of the physically cross-linked membranes were measured by TGA with different membranes' composition as PVA: Cs-g-GTMAC, where the TGA thermographs' chart is shown in Figure 7 while summarized TGA data are listed in Table 2. As clearly seen, the incorporation of Cs-g-GTMAC at different ratios (0%, 10%, 20%, and 30%) into the PVA hydrogel membranes significantly enhanced $T_{onset}$ from 234°C to 247°C. Also, the incorporation of Cs-g-GTMAC into the PVA hydrogel membranes prolonged the decomposition temperature of the half-weight loss % ($T_{50\%}$) from 345°C to 361°C. On the other side, the incorporation of Cs-g-GTMAC into the PVA hydrogel membranes progressively improved and was thermally delayed from 350°C to 396°C (Table 2, pyrolysis third decomposition stage). These findings are consistent with the obtained results of Kamoun *et al*. (2015a) and Kenawy *et al*. (2014). They proved that the incorporation of HES or sodium alginate into physically cross-linked PVA hydrogel membranes significantly enhanced the thermal properties of entangled composite membranes.

## Bioevaluation tests

### *Antimicrobial activity test*

The antibacterial activity of the PVA-Cs-g-GTMAC-Ag membranes against *E. coli* and *S. aureus* is summarized in Table 3. The inhibitory effect of the PVA-Cs-g-GTMAC-Ag membranes versus *E. coli* and *S. aureus* is higher versus *S. aureus* than *E. coli,* perhaps owing to the alteration in their cell-wall composition. It is observed that the inhibition zone increased significantly with increasing the GTMAC content in the tested membrane disks. The antibacterial activities of Cs and Ag NPs have already been studied by many scientists (Chi *et al*., 2007; Kim *et al*., 2007; Wei *et al*., 2009), where the antibacterial activity of Cs-Ag (silver ions or NPs) was found to be higher than each component of the membrane (Wei *et al*., 2009). The mechanism of action is based on the Cs binding with microbial DNA, which leads to inhibiting of mRNA and protein synthesis *via* penetration of Cs into the nuclei of microorganisms (Sebti *et al*., 2005).

Cs after quaternization comes to be a very water-soluble polyelectrolyte polysaccharide with a high charge density (Muzzarelli *et al*., 1990). Polycationic biocidal agents can interact and form polyelectrolyte complexes with acidic polymers, which form on the surface of the bacterial cells. The target site of the cationic antibacterial agents is the negatively charged cell surface of bacteria (Chi *et al*., 2007). Also, the antibacterial activity of silver NPs is well known to be highly reactive because of their large surface area; thus, they might be more efficient in their antimicrobial activities (Gogoi *et al*., 2006). The antimicrobial mechanism of silver NPs is ascribed to the free radical formation, which causes damage to the bacterial membrane, leading to cell death (Kim *et al*., 2007). Ag NPs attach to the cell membrane and disturb its vital functions, e.g., permeability and respiration; furthermore, Ag NPs are capable

of penetrating the bacterial cell wall causing significant cell wall damage due to interacting with sulfur- and phosphorus-containing DNA (Wei *et al*., 2009). These results are confirmed by those obtained by Cheah et al. (2019), where the antibacterial activity of quaternized Cs NFs was found to be higher than the Cs modified membrane against *E. coli* and also those obtained by Archana *et al*. (2015). Similarly, $Ag_2O$ NPs-loaded-Cs-PVP films showed high antibacterial activity since both Cs and $Ag_2O$ NPs possess a remarked antibacterial activity (Archana *et al*., 2015; Cheah *et al*., 2019).

***In vitro cell viability (%) test by MTT assay***

As it is important to test the safety and compatibility of the prepared polymeric compounds of PVA, Ag, Cs, and GTMAC in biological application uses, MTT assays on human HFB-4 normal skin melanocyte cells were carried out (Fig. 8). Our results revealed avoidance in the cytotoxicity of HFB-4 cells with all the prepared polymeric compounds as compared to the untreated cells. The maximum obtained toxicity was observed with all compounds at 5.0 mg/ml after 6 days incubation with viability around 90%. On the other hand, the viability of the HFB-4 cells reached values around 100%, with concentrations of 1.0, 2.0, and 3.0 mg/ml after incubation for all tested times. The efficiency of the encapsulation method of Ag, Cs, and GTMAC within the PVA polymer is evident from these findings, and this might lead to reducing their cytotoxicity without decreasing in the used doses. It was also perceived that the cytotoxicity of PVA-Cs-g-GTMAC-Ag (90:10) was less than PVA-Cs-g-GTMAC-Ag (80:20) and PVA-Cs-g-GTMAC-Ag (70:30) against the HFB-4 cells than PVA only. This slight toxicity effect might be attributed to the increasing content of Ag in polymer complexes. These findings agreed with those reported by Wu *et al*. (2021). They proved that a quaternized Cs/PVA nanofiber membrane cross-linked with blocked diisocyanate has a potential skin regeneration ability as a wound dressing and a very low cytotoxic prepared nanofiber on mouse fibroblasts (Wu *et al*., 2021).

## CONCLUSION

PVA-Cs-g-GTMAC-Ag composed hydrogel membranes were physically cross-linked and prepared for antibacterial wound dressing biomaterials. Instrumental characterization, e.g., FT-IR, TGA, TEM, and SEM analyses, was employed to verify the chemical structure, thermal stability, and surface morphology, respectively, for the prepared PVA-Cs-g-GTMAC-Ag composed hydrogel membranes. The physicochemical and mechanical properties of the composite membranes were also discussed to explore the influence of varied hydrogel compositions on either the PVA or GTMAC contents in the obtained hydrogel membranes. The prepared composite hydrogel membranes showed a promising antibacterial activity against both G+ and G− *bacteria* with increasing the GTMAC content. Moreover, biodegradability, blood compatibility, and cellular toxicity results explored that the novel synthesized PVA-Cs-g-GTMAC-Ag composite hydrogel membranes are regarded as promising biomaterials and are good antibacterial, biodegradable, and nontoxic biomaterial candidates for topical wound healing purposes.

## ACKNOWLEDGMNTS

The authors would like to thank Tanta University for financial support through project ID TU:03-19-02, “Preparation of novel antimicrobial polymeric membranes for wound healing applications.”

## CONFLICT OF INTEREST

The authors declare no competing or financial interests.

## AUTHOR CONTRIBUTIONS

All authors made substantial contributions to conception and design, acquisition of data, or analysis and interpretation of data; took part in drafting the article or revising it critically for important intellectual content; agreed to submit to the current journal; gave final approval of the version to be published; and agree to be accountable for all aspects of the work. All the authors are eligible to be an author as per the international committee of medical journal editors (ICMJE) requirements/guidelines.

## ETHICAL APPROVALS

This study does not involve experiments on animals or human subjects.

## DATA AVAILABILITY

All data generated and analyzed are included within this research article.

## PUBLISHER’S NOTE

This journal remains neutral with regard to jurisdictional claims in published institutional affiliation.

## REFERENCES

Abdelaal MY, Sobahi TR, Al-Shareef HF. Modification of chitosan derivatives of environmental and biological interest: a green chemistry approach. Inter J Biolog Macromol, 2013; 55:231–9.

Afshar M, Dini G, Vaezifar S, Mehdikhani M, Movahed B. Preparation and characterization of sodium alginate/polyvinyl alcohol hydrogel containing drug-loaded chitosan nanoparticles as a drug delivery system. J Drug Deliv Sci Technol, 2020; 56:101530.

Al Ghamdi YO, Alamry KA, Asiri AM, Hussein MA. Recent trends on chemically modified chitosan for biological interest . MedCrave Group LLC., 2017.

Archana D, Singh BK, Dutta J, Dutta PK. Chitosan-PVP-nano silver oxide wound dressing: in vitro and *in vivo* evaluation. Inter J Biolog Macromol, 2015; 73:49–57.

Cai J, Dang Q, Liu C, Wang T, Fan B, Yan J, Xu Y. Preparation, characterization and antibacterial activity of O-Acetyl-Chitosan-N-2-hydroxypropyl trimethyl ammonium chloride. Inter J Biolog Macromol, 2015; 80:8–15.

Caló E, Khutoryanskiy VV. Biomedical applications of hydrogels: a review of patents and commercial products. Europ Polym J, 2015; 65:252–67.

Cheah WY, Show PL, Ng IS, Lin GY, Chiu CY, Chang YK. Antibacterial activity of quaternized chitosan modified nanofiber membrane. Inter J Biolog Macromol, 2019; 126:569–77.

Chi W, Qin C, Zeng L, Li W, Wang W. Microbiocidal activity of chitosan-N-2-hydroxypropyl trimethyl ammonium chloride. J Applied Polym Sci, 2007; 103(6):3851–6.

El-Fakharany EM, Abu-Elreesh GM, Kamoun EA, Zaki S, Abd-EL-Haleem DA. In vitro assessment of the bioactivities of sericin protein extracted from a bacterial silk-like biopolymer. RSC Adv, 2020; 10(9):5098–107.

Figueroa-Pizano MD, Vélaz I, Peñas FJ, Zavala-Rivera P, Rosas-Durazo AJ, Maldonado-Arcee AD, Martínez-Barbosa ME. Effect of freeze-thawing conditions for preparation of chitosan-poly (vinyl alcohol)

hydrogels and drug release studies. Carbohyd Polym, 2018; 195:476–85.

Gogoi SK, Gopinath P, Anumita P, Ramesh A, Ghosh SS, Chattopadhyay A. Green fluorescent protein-expressing *Escherichia coli* as a model system for investigating the antimicrobial activities of silver nanoparticles. Langmuir, 2006; 22(22):9322–8.

Hassan A, Niazi MBK, Hussain A, Farrukh S, Ahmad T. Development of anti-bacterial PVA/starch based hydrogel membrane for wound dressing. J Polym Enviro, 2018a; 26(1):235–43.

Hassan MA, Omer AM, Abbas E, Baset WMA, Tamer TM. Preparation, physicochemical characterization and antimicrobial activities of novel two phenolic chitosan Schiff base derivatives. Scient Rep, 2018b; 8(1):1–14.

Jin Y, Dong S. One-pot synthesis and characterization of novel silver−gold bimetallic nanostructures with hollow interiors and bearing nanospikes. J Physical Chem B, 2003; 107(47):12902–5.

Kamel GM, El-Nahass MN, El-Khouly ME, Fayed TA, El-Kemary M. Simple, selective detection and efficient removal of toxic lead and silver metal ions using Acid Red 94. RSC Adv, 2019; 9(15):835–63.

Kamoun EA, Menzel H. HES-HEMA nanocomposite polymer hydrogels: swelling behavior and characterization. J Polym Res 2012; 19(4):9851.

Kamoun E, Fahmy A, El-Dmahougy BK. Synthesis and characterization of poly (vinyl alcohol)-hyaluronic acid blended hydrogel membranes. J Pharma Sci, 2014; 49(1):183–93.

Kamoun EA, Chen X, Mohy Eldin MS, Kenawy ES. Crosslinked poly (vinyl alcohol) hydrogels for wound dressing applications: a review of remarkably blended polymers. Arab J Chem, 2015a; 8(1):1–14.

Kamoun EA, Kenawy ES, Tamer TM, El-Meligy, MA, Mohy Eldin MS. Poly (vinyl alcohol)-alginate physically crosslinked hydrogel membranes for wound dressing applications: characterization and bio-evaluation. Arab J Chem, 2015b; 8(1):38–47.

Kamoun EA, Kenawy ES, Chen X. A review on polymeric hydrogel membranes for wound dressing applications: PVA-based hydrogel dressings. J Adv Res, 2017; 8(3):217–33.

Kenawy ES, Kamoun EA, Mohy Eldin MS, El-Meligy, MA. Physically crosslinked poly (vinyl alcohol)-hydroxyethyl starch blend hydrogel membranes: Synthesis and characterization for biomedical applications. Arab J Chem, 2014; **7**(3):372–80.

Kenawy E, Omar AM, Tamer TM, El-Meligy MA. Fabrication of biodegradable gelatin/chitosan/cinnamaldehyde crosslinked membranes for antibacterial wound dressing applications. Inter J Biolog Macromol, 2019; 139:440–8.

Kim JS, Kuk E, Yu KN, Kim JH, Park SJ, Lee HJ, Kim SH, Park YK, Park YH, Hwang CY, Kim YK, Lee YS, Jeong DH, Cho MH. Antimicrobial effects of silver nanoparticles. Nanomedicine, 2007; 3(1):95–101.

Liu P. Quaternary ammonium salt of chitosan: preparation and antimicrobial property for paper. Open Med, 2015; 10(1):473–8.

Martins AF, Facchi SP, Follmann HDM, Pereira AGB, Rubira AF, Muniz EC. Antimicrobial activity of chitosan derivatives containing N-quaternized moieties in its backbone: a review. Inter J Molecular Sci, 2014; 15(11):20800–32.

Mosmann T. Rapid colorimetric assay for cellular growth and survival: application to proliferation and cytotoxicity assays. J Immunol Meth, 1983; 65(1-2):55–63.

Muzzarelli R, Tarsi R, Filippini O, Giovanetti E, Biagini G, Varaldo PE. Antimicrobial properties of N-carboxybutyl chitosan. Antimicrob Agent Chemother, 1990; 34(10):2019–23.

Paladini F, Pollini M. Antimicrobial silver nanoparticles for wound healing application: progress and future trends. Materials, 2019; 12(16):2540.

Sebti I, Martial-Gros A, Carnet-Pantiez A, Grelier S, Coma V. Chitosan polymer as bioactive coating and film against *Aspergillus niger* contamination. J Food Sci, 2005; 70(2):M100–4.

Shariatinia Z, Jalali AM, Chitosan-based hydrogels: preparation, properties and applications. Inter J Biolog Macromol, 2018; 115:94–220.

Simões D, Miguel SP, Ribeiro MP, Coutinho P, Mendonça AG, Correia IG. Recent advances on antimicrobial wound dressing: a review. Europ J Pharma Biopharma, 2018; 127:130–41.

Suhas K, Manvi PMN. Efficacy of nano silver dressings over conventional dressings in chronic wounds. Intern Surgery J, 2018; 5(12):3995–9.

Tang Y, Lan X, Liang C, Zhong Z, Xie R, Zhou Y, Miao X, Wang H, Wang W. Honey loaded alginate/PVA nanofibrous membrane as potential bioactive wound dressing. Carbohydrate Polym, 2019; 219:113–20.

Valgas C, Machado de Souza S, Smânia EFA, Jr AS. Screening methods to determine antibacterial activity of natural products. Brazil J Microbiol, 2007; 38(2):369–80.

Vinsova J, Vavrikova E. Chitosan derivatives with antimicrobial, antitumor and antioxidant activities-a review. Curr Pharma Design, 2011; 17(32):3596–607.

Wei D, Sun W, Qian W, Ye Y, Ma X. The synthesis of chitosan-based silver nanoparticles and their antibacterial activity. Carbohydrate Res, 2009; 344(17):2375–82.

Wilkinson L, White R, Chipman J. Silver and nanoparticles of silver in wound dressings: a review of efficacy and safety. J Wound Care, 2011; 20(11):543–9.

Wu JY, Ooi CW, Song CP, Wang CY, Liu BL, Lin GY, Chiu CY, Chang YK. Antibacterial efficacy of quaternized chitosan/poly (vinyl alcohol) nanofiber membrane crosslinked with blocked diisocyanate. Carbohydrate Polym, 2021; 262:117910.

Xiao C, Zhou G. Synthesis and properties of degradable poly (vinyl alcohol) hydrogel. Polym Deg Stability, 2003; 81(2):297–301.

Yang X, Liu Q, Chen X, Yu F, Zhu Z. Investigation of PVA/ws-chitosan hydrogels prepared by combined γ-irradiation and freeze-thawing. Carbohydrate Polym, 2008a; 73(3):401–8.

Yang SL, Wu ZH, Yang W, Yang MB. Thermal and mechanical properties of chemical crosslinked polylactide (PLA). Polymer Testing, 2008b; 27(8):957–63.

Zhao L, Mitomo H, Zhai M, Yoshii F, Nagasawa N, Kume T. Synthesis of antibacterial PVA/CM-chitosan blend hydrogels with electron beam irradiation. Carbohydrate Polym, 2003; 53(4):439–46.

**How to cite this article:**
Kenawy ES, Kamoun EA, Elsigeny SM, Haikal S, El-Shehawy AA, Mahmoud YAG. Physically crosslinked PVA-quaternized chitosan-Ag NPs composite hydrogel membranes for potential topical wound healing applications: Synthesis, physicochemical properties, and *in vitro* bioevaluation. J Appl Pharm Sci, 2023; 13(03):023–035.

## SUPPLEMENTARY MATERIAL

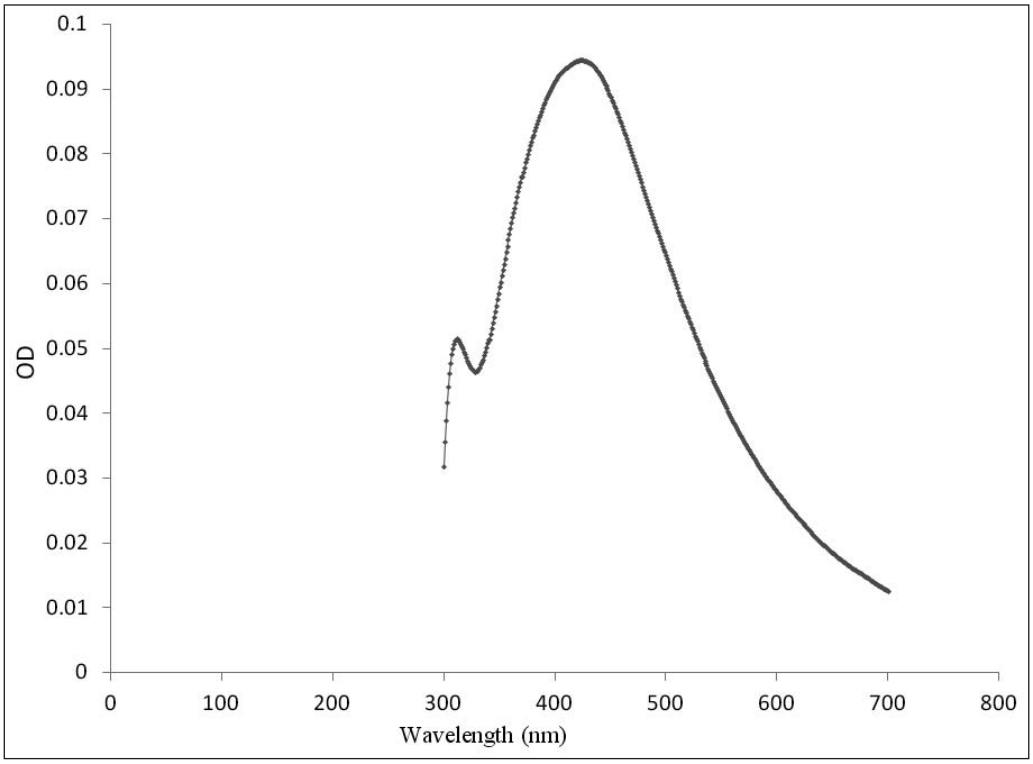


**Figure S1.** UV analysis of Ag nanoparticles.

**GRAPHICAL ABSTRACT**